Balkan Med J 2026;43:196-205



# Significance of LEF1, ROR2, Cyclin D1, and DNA Methylation Profiling in the Molecular Classification and Prognosis Prediction of Pediatric Medulloblastoma

Mehmet Fatih Tekin[1,2], Dilek Gül[3], Nurşah Eker[4], Adnan Dağçınar[5], Yaşar Bayri[5], Fatih Bayraklı[5], Beste Melek Atasoy[6], Süheyla Uyar Bozkurt[1,7]

[1]Department of Pathology, Marmara University Faculty of Medicine, İstanbul, Türkiye
[2]Department of Pathology, Marmara University Pendik Training and Research Hospital, İstanbul, Türkiye
[3]Department of Radiation Oncology, Marmara University Pendik Training and Research Hospital, İstanbul, Türkiye
[4]Department of Pediatric Hematology and Oncology, Marmara University Faculty of Medicine, İstanbul, Türkiye
[5]Department of Neurosurgery, Marmara University Faculty of Medicine, İstanbul, Türkiye
[6]Department of Radiation Oncology, Marmara University Faculty of Medicine, İstanbul, Türkiye
[7]Department of Pathology, İstinye University Faculty of Medicine, İstanbul, Türkiye

**Background:** Accurate identification of medulloblastoma molecular subgroups is essential, particularly in settings lacking advanced genomic tools. Conventional markers, such as β-catenin, present significant challenges in reliably detecting the WNT-activated subgroup (WNT-AG).

**Aims:** To evaluate the utility of lymphoid enhancer-binding factor 1 (LEF1), Cyclin D1, and receptor tyrosine kinase-like orphan receptor 2 (ROR2) as immunohistochemical (IHC) markers for molecular subgroup classification and to assess their prognostic significance.

**Study Design:** Retrospective cohort study.

**Methods:** IHC analysis was performed using LEF1, Cyclin D1, and ROR2. Two distinct LEF1 staining patterns were identified: nuclear (nLEF1) and punctate (pLEF1). A subset of 29 cases, selected based on predefined criteria, underwent EPIC array Methylation analysis. Findings were correlated with recurrence and survival outcomes.

**Results:** Among the 94 cases, 12.8% were WNT-AG, 54.3% were sonic hedgehog-activated subgroup (SHH-AG), and 33.0% were Groups 3 and 4 (G3/4). nLEF1 demonstrated higher specificity and sensitivity for WNT-AG than β-catenin, identifying it as a more reliable diagnostic marker. High pLEF1 expression was strongly associated with SHH-AG. Cyclin D1 positivity was predominantly observed in WNT-AG. While ROR2 did not identify WNT-AG effectively, its absence in Group 3 cases was notable. Prognostic analysis revealed that LEF1 expression patterns correlated with favorable survival outcomes: total LEF1 (tLEF1) and nLEF1 were associated with improved overall survival, whereas pLEF1 and tLEF1 were linked to better progression-free survival.

**Conclusion:** Nuclear LEF1 (nLEF1) is at least as effective as β-catenin in identifying WNT-AG and may serve as a superior diagnostic marker. Cyclin D1 can be used as a complementary marker in WNT-AG detection. ROR2 negativity may indicate G3 tumors, though further studies are warranted to confirm its prognostic value.

**Corresponding author:** Mehmet Fatih Tekin, Department of Pathology, Marmara University Faculty of Medicine; Marmara University Pendik Training and Research Hospital, İstanbul, Türkiye

**e-mail:** mfatihtekinmd@gmail.com

**Received:** October 09, 2025 **Accepted:** December 30, 2025 **Available Online Date:** April 1, 2026 • **DOI:** 10.4274/balkanmedj.galenos.2025.2025-10-51

Available at www.balkanmedicaljournal.org

**ORCID iDs of the authors:** M.F.T. 0000-0002-3998-2860; D.G. 0000-0003-0382-8842; N.E. 0000-0002-7707-3035; A.D. 0000-0001-9532-7820; Y.B. 0000-0003-0668-5453; F.B. 0000-0003-1707-6055; B.M.A. 0000-0003-1320-9105; S.U.B. 0000-0002-5947-947X.

**Cite this article as:** Tekin MF, Gül D, Eker N, et al. Significance of LEF1, ROR2, Cyclin D1, and DNA Methylation Profiling in the Molecular Classification and Prognosis Prediction of Pediatric Medulloblastoma. Balkan Med J. 2026;43:196-205

## INTRODUCTION

Medulloblastoma is the second most common pediatric central nervous system (CNS) tumor after high-grade gliomas, accounting for approximately 20% of intracranial neoplasms in children.[1] It is the most frequently encountered embryonal CNS tumor. According to the 5th edition of the World Health Organization Classification of CNS Tumors, medulloblastomas are divided into four molecular groups:[2] sonic hedgehog (SHH)-activated subgroup (SHH-AG; *TP53* mutant and non-*TP53* mutant), wingless/INT1 (WNT)-activated subgroup (WNT-AG), Group 3 (G3), and Group 4 (G4). When a clear distinction between G3 and G4 cannot be established, they are collectively classified as non-WNT/non-SHH or G3/4.

These molecular subgroups are critical for understanding disease pathogenesis, guiding targeted therapies, and predicting prognosis. The gold standard for subgroup determination involves genetic analyses, including whole-genome sequencing or DNA methylation profiling. However, these techniques are restricted to specialized centers due to high costs and the requirement for trained personnel. In settings where genetic testing is unavailable, immunohistochemistry (IHC) is commonly used for classification. Nuclear β-catenin (β-catenin) positivity is the most widely applied IHC marker for identifying activation of the WNT signaling pathway. Nevertheless, diagnostic challenges arise when cytoplasmic staining is intense or nuclear staining is sparse and limited to a few cells. This limitation has prompted pathologists to explore alternative markers, informed by an expanded understanding of the WNT pathway.

The WNT signaling pathway comprises canonical and non-canonical branches. The canonical pathway is β-catenin dependent, whereas non-canonical pathways include the planar cell polarity pathway, calcium-dependent pathway, WNT/RAP1, WNT/ROR, WNT/PKA, WNT/PKC, and WNT/mechanistic target of rapamycin pathways.[3,4]

In the final step of the canonical WNT pathway, β-catenin translocates to the nucleus, where it binds to T-cell factor/lymphoid enhancer-binding factor 1 (LEF1) and activates the transcription of target genes such as *Cyclin D1, myelocytomatosis oncogene,* and *Axin2*, thereby initiating tumorigenesis. In the WNT/ROR non-canonical pathway, the WNT ligand binds to receptor tyrosine kinase-like orphan receptor 2 (ROR2), triggering cell proliferation.[3,5,6]

This study aimed to accurately differentiate the molecular subgroups of medulloblastoma and to explore additional parameters that could support histomorphological and IHC methods used for prognostication. Furthermore, it sought to identify WNT-AG tumors using a method more reliable than the conventional β-catenin marker.

Specifically, the study evaluated the roles of ROR2 and LEF1 in identifying WNT-AG tumors and their association with prognosis. It also investigated the relationship between Cyclin D1 expression, molecular subgroups, and clinical outcomes. Finally, "EPIC array" methylation analysis was applied to a representative sample set encompassing all molecular subgroups to assess the correlation between routine methods and methylation results as well as the association of newly investigated markers with molecular subgroup classification.

## MATERIALS AND METHODS

This study was approved by the Clinical Research Ethics Committee of the Faculty of Medicine, Marmara University (approval number: 09.2021.1253; date: 05.11.2021). The requirement for informed consent was waived due to the retrospective nature of the study.

A total of 94 medulloblastoma samples were collected from the Department of Pathology between January 2011 and January 2024. All pediatric cases received during this period with sufficient tissue in formalin-fixed, paraffin-embedded (FFPE) blocks were included. Histopathological review was independently performed by two pathologists, one of whom is a neuropathology specialist.

Demographic and radiological data were obtained from the hospital information system. Clinical information, including residual disease, recurrence, metastasis, initial and final follow-up dates, and disease progression, was retrieved from patient records in the Pediatric Oncology and Radiation Oncology departments. Survival outcomes were verified using the death notification system of the Ministry of Health.

### *Immunohistochemistry*

Based on tissue adequacy in the FFPE samples, Grb2-associated binding protein 1 (GAB1) and β-catenin were evaluable in 94 cases; Cyclin D1, yes-associated protein 1 (YAP1), Ki-67, and p53 in 93 cases; LEF1 in 92 cases; and ROR2 in 88 cases (Tables 1 and 2). Slides archived in the department were used to assess GAB1, YAP1, β-catenin, Ki-67, and p53.

Sections (2 µm) from FFPE blocks were mounted on electrostatically charged slides and dried for at least 1 hour at 72 °C. Cyclin D1 (Biocare, EP12, 1:100) and LEF1 (Medaysis, B6, 1:200) were processed using a Ventana BenchMark Ultra system (Ventana Medical Systems, Tucson, AZ), including deparaffinization and antigen retrieval, with the ready-to-use Ultraview™ Universal DAB Detection Kit (Cat. No. 760-500). Counterstaining with hematoxylin, bluing, dehydration, xylene clearing, and coverslipping were performed manually.

ROR2 immunostaining employed the AMAb91402-25 µL ROR2 (CL5950) antibody (Sigma-Aldrich/Atlas, Bromma, Sweden) at a 1:500 dilution with 120-minute incubation. Detection was enhanced using a signal-amplification kit. Antigen retrieval followed the standard ROCHE CC1 (EDTA) protocol for 90 minutes, and secondary detection was performed with the ROCHE UltraView Universal DAB Kit on a Ventana BenchMark XT IHC stainer according to standard procedures.

Within the tumor area, ROR2, LEF1, Cyclin D1, GAB1, YAP1, β-catenin, Ki-67, and p53 staining was evaluated. LEF1 was considered positive when nuclear staining was observed, and two distinct patterns were recorded. For cases with uniform, strong nuclear staining, a nuclear LEF1 (nLEF1) score was assigned. When punctate, scattered nuclear staining was present, a punctate LEF1 (pLEF1) score was applied. Regardless of the pattern, a total-LEF1 (tLEF1) score was determined for all nLEF1 staining (Figure 1).

ROR2 staining was predominantly observed in areas of neurocytic differentiation, such as within nodules. Scores encompassing all ROR2 staining were defined as total ROR2 (tROR2), whereas scores excluding intranodular areas were recorded as corrected ROR2 (cROR2).

When evaluating ROR2, LEF1, Cyclin D1, GAB1, and YAP1 staining, the degree of immunoreactivity was scored on a scale from 0 to 3 (0: no staining; 1: mild; 2: moderate; 3: strong) (Figures 2-4). The proportion of the tumor area exhibiting each staining intensity was calculated. The Histoscore (H-score) was then determined by multiplying the staining intensity by the corresponding percentage of tumor area, yielding a semiquantitative score ranging from 0 to 300 (0 for completely negative cases and 300 if all tumor cells showed 3+ staining).[7]

Stains were also categorized as positive (H-score > 0) or negative (H-score = 0). Nuclear staining of tumor cells with β-catenin was considered positive regardless of the proportion of stained cells.[2]

Ki-67 labeling was assessed manually by estimating the percentage of positive cells within the hot-spot area under high-power magnification.[8] p53 staining was analyzed as a continuous variable; additionally, using a 50% cut-off, cases were classified as positive or negative.[9,10] No cases exhibited complete absence of p53 staining (null type).

### EPIC array methylation analysis

Genomic DNA was isolated from FFPE samples using the ReliaPrep FFPE gDNA Miniprep System (#A2352). DNA concentration was measured, followed by quality assessment using the Infinium FFPE QC Kit (#WG-321-1001) to confirm suitability for downstream analysis. Samples meeting the required quality criteria were subjected to bisulfite conversion using 500 ng of DNA per sample, performed with the EZ DNA Methylation Kit (#D5001). Because bisulfite treatment significantly alters the physical and chemical properties of DNA, the treated DNA was subsequently cleaned and

**TABLE 1.** Median Values of Ki-67 and p53 Percentages Across Molecular Groups and Corresponding *p* values.

| | Ki67 | | p53 | |
|---|---|---|---|---|
| | Median (min-max) | *p* value | Median (min-max) | *p* value |
| WNT-AG | 75.0 (40.0-95.0) | 0.091 | 27.5 (2.0-80.0) | 0.262 |
| SHH-AG | 60.0 (10.0-90.0) | | 5.0 (1.0-95.0) | |
| G3/4 | 70.0 (15.0-95.0) | | 5.0 (1.0-80.0) | |

WNT-AG, WNT activated group; SHH-AG, SHH activated group; G3/4, group 3 and group 4.

**TABLE 2.** Positivity Status of LEF1, ROR2, Cyclin D1, GAB1 and β-catenin Markers According to Molecular Groups.

| | | WNT-AG (n) | SHH-AG (n) | G3/4 (n) | Total (n) | n |
|---|---|---|---|---|---|---|
| tLEF1 | (+) | 11 | 31 | 13 | 55 | 92 |
| | (-) | 0 | 20 | 17 | 37 | |
| nLEF1 | (+) | 11 | 2[b] | 1[a] | 14 | 92 |
| | (-) | 0 | 49 | 29 | 78 | |
| pLEF1 | (+) | 9 | 31 | 13 | 53 | 92 |
| | (-) | 2 | 20 | 17 | 39 | |
| tROR2 | (+) | 9 | 45 | 19 | 73 | 88 |
| | (-) | 1 | 4 | 10 | 15 | |
| cROR2 | (+) | 9 | 42 | 19 | 70 | 88 |
| | (-) | 1 | 7 | 10 | 18 | |
| Cyclin D1 | (+) | 11 | 22 | 9 | 42 | 93 |
| | (-) | 1 | 29 | 21 | 51 | |
| GAB1 | (+) | 8[a] | 50 | 6[a] | 64 | 94 |
| | (-) | 4 | 1[a] | 25 | 30 | |
| β-catenin | (+) | 10 | 3 | 1 | 14 | 94 |
| | (-) | 2[a] | 48 | 30 | 80 | |

LEF1, lymphoid enhancer-binding factor; tLEF1, total LEF1; nLEF1, nuclear LEF1; pLEF1, punctate LEF1; ROR2, receptor tyrosine kinase-like orphan receptor 2; tROR2, total ROR2; cROR2, corrected ROR2; WNT-AG, WNT activated group; SHH-AG, SHH activated group; G3/4, group 3 and group 4.
[a]Confirmed by methylation analysis.
[b]The calibration score during methylation analysis of two cases diagnosed with SHH-AG was 0.38.

restored using the ZR-96 DNA Clean & Concentrator-5 (#D4023) and the Infinium HD FFPE DNA Restore Kit (24 samples, #WG-321-1002) to ensure compatibility with array analysis.

Prepared DNA samples then underwent amplification, hybridization, and staining prior to scanning. Samples were loaded onto MethylationEPIC BeadChips and scanned using the Illumina iScan system to assess genome-wide methylation profiles. This approach analyzed over 850,000 methylation sites across the genome. The resulting IDAT files were processed using the methylation module of Illumina GenomeStudio v2011.

In total, EPIC array methylation analysis was performed on 29 cases. Cases were selected to classify immunohistochemically unclassified medulloblastomas (medulloblastoma-NOS) and to clarify the molecular classification of tumors with uncertain or potentially nuclear β-catenin staining. This strategy ensured adequate representation of WNT-AG tumors, as cases with equivocal β-catenin staining were retained. Additionally, cases exhibiting variable LEF1, ROR2, and Cyclin D1 expression were included to capture the natural spectrum of staining intensities (low, moderate, high) observed in the cohort.

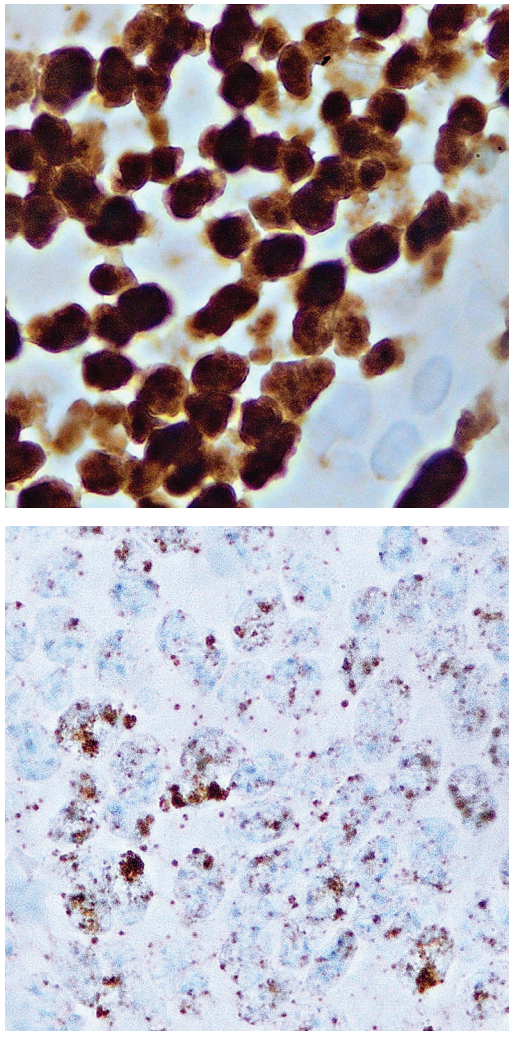


**FIG. 1.** Lymphoid enhancer-binding factor 1 (LEF1). Staining patterns (x100). Strong and nuclear (nLEF1) (a). Punctate nuclear (pLEF1) (b).

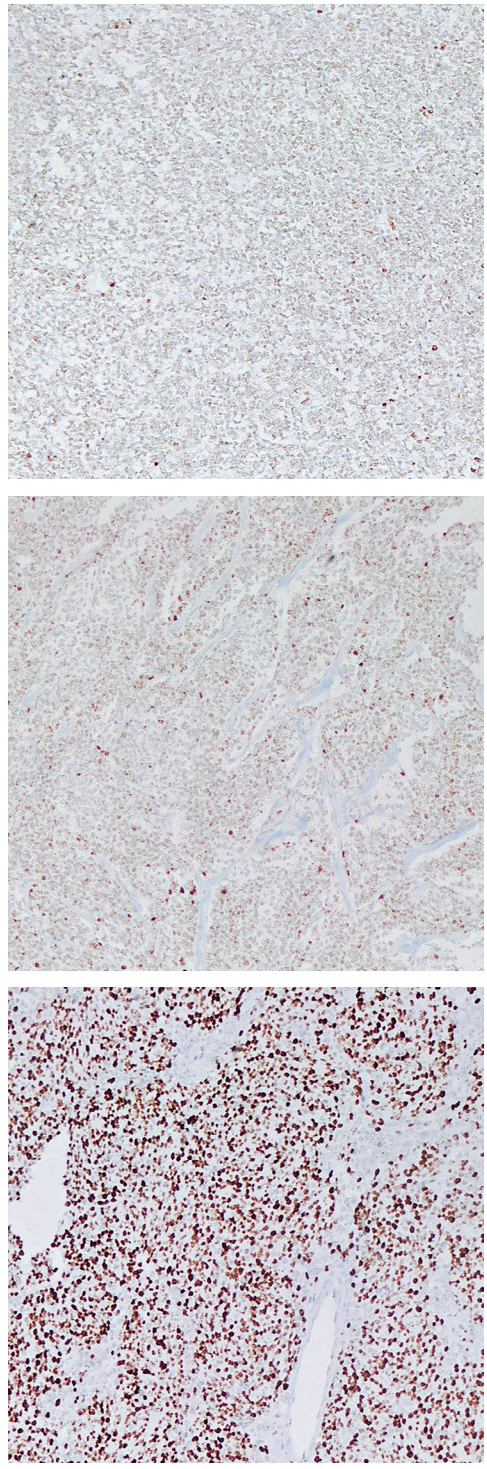


**FIG. 2.** Lymphoid enhancer-binding factor 1 immunohistochemical staining scores (×10). Score 1, mild staining intensity (a). Score 2, moderate staining intensity (b). Score 3, strong staining intensity (c).

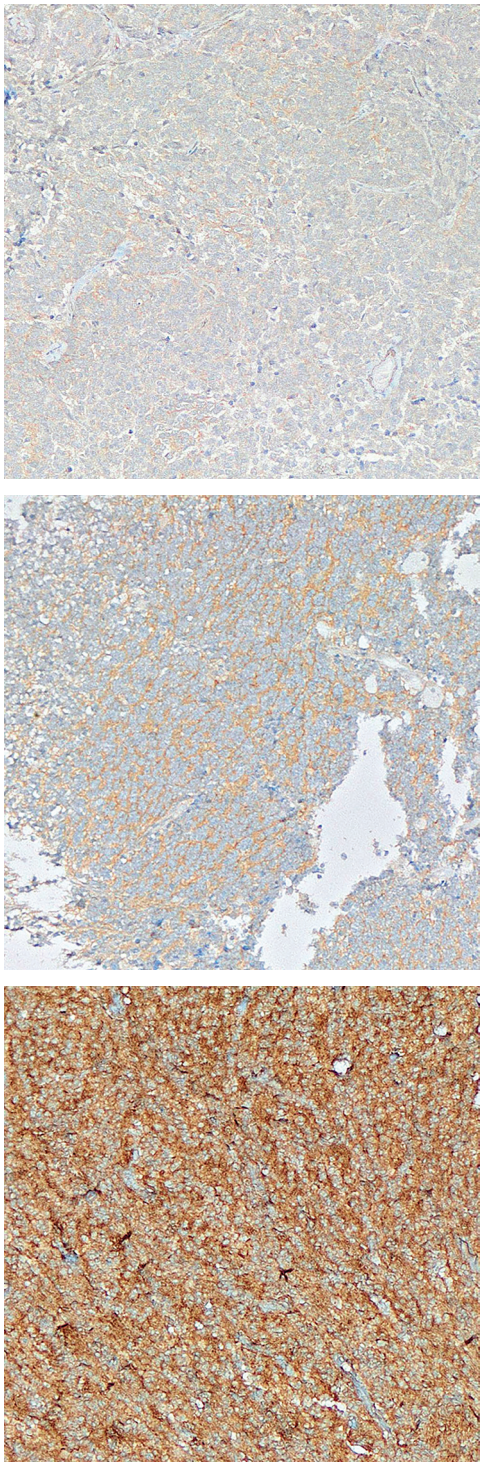


**FIG. 3.** Receptor tyrosine kinase-like orphan receptor 2 immunohistochemical staining scores (×10). Score 1, mild staining intensity (a). Score 2, moderate staining intensity (b). Score 3, strong staining intensity (c).

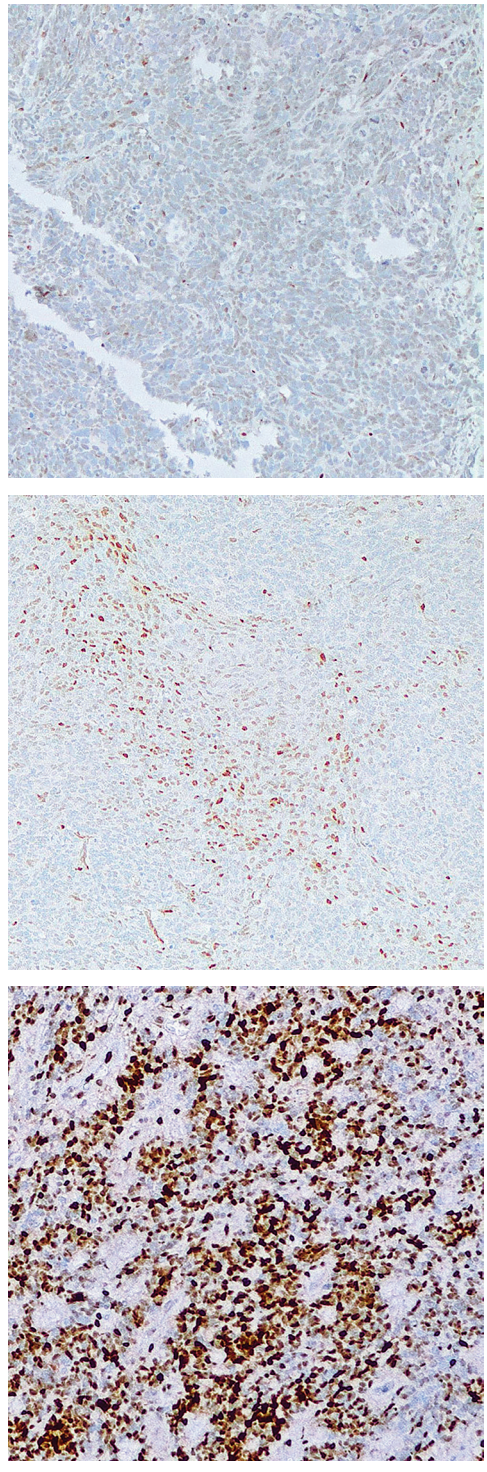


**FIG. 4.** Cyclin D1 immunohistochemical staining scores (×10). Score 1, mild staining intensity (a). Score 2, moderate staining intensity (b). Score 3, strong staining intensity (c).

Methylation data from the 29 cases were uploaded to a secure, internationally recognized database and compared against reference dataset version 12.8. Cases with a calibration score ≥ 0.9 were considered consistent with the molecular group and subgroup assigned by the system.

### Statistical analysis

Statistical analyses were performed using IBM SPSS Statistics version 26.0. Categorical variables were analyzed using Pearson's chi-square, Yates' chi-square, and Fisher's exact tests. Comparisons of continuous variables were conducted using the Mann–Whitney U and Kruskal–Wallis tests, while Spearman's correlation was used to assess associations between variables. Receiver operating characteristic curve analysis was applied to determine optimal cut-off values.

Survival outcomes were evaluated using Kaplan–Meier analysis and the log-rank test, and multivariate analyses were conducted using the Cox proportional hazards regression model to identify independent prognostic factors. A $p$ value $< 0.05$ was considered statistically significant.

Given the fixed sample size of this retrospective study, a sensitivity analysis was performed. With $\alpha = 0.05$ and 80% statistical power, the study was sufficiently powered to detect moderate effect sizes (Cohen's $f \approx 0.35$; $w \approx 0.30$), based on parametric equivalents of the non-parametric tests applied.

## RESULTS

A total of 94 medulloblastoma cases were included in this study. Of these, 62 (65.96%) were male and 32 (34.04%) were female, yielding a male-to-female ratio of 1.94. The median age at diagnosis was 6 years (range: 1–16 years).

Molecular subgroup classification identified 12 cases (12.77%) as WNT-AG, 51 cases (54.26%) as SHH-AG, and 31 cases (32.98%) as G3/4. Analysis of age at diagnosis revealed that WNT-AG cases were diagnosed at a significantly older age compared to the other subgroups ($p = 0.015$). No significant association was observed between molecular subgroup and gender.

### Association between molecular subgroups and immunohistochemistry stains

The H-score of GAB1 was significantly higher in SHH-AG tumors compared to other subgroups, whereas it was markedly lower in G3/4 tumors ($p < 0.001$). The H-score of YAP1 was also reduced in G3/4 ($p = 0.006$). No significant differences were observed in the percentages of Ki-67 and p53 staining among molecular subgroups (Table 1).

In cases with practical difficulties in molecular subgroup identification, GAB1, a marker indicative of SHH-AG, was variably positive in 8 of 12 WNT-AG cases (66.7%) and 6 of 31 G3/4 cases (19.4%). β-catenin staining was negative in 2 of 12 WNT-AG cases (16.7%). Conversely, β-catenin positivity was observed in 3 of 51 SHH-AG cases (5.9%) and 1 of 31 G3/4 cases (3.2%) (Table 2).

The H-scores for tLEF1, nLEF1, and pLEF1 were significantly higher in WNT-AG cases ($p < 0.001$). When WNT-AG cases were excluded, pLEF1 H-scores were significantly higher in SHH-AG tumors compared to G3/4 ($p = 0.039$).

Optimal cut-off values for LEF1 expression in identifying WNT-AG were relatively low (nLEF1 = 2.50, J = 0.975; pLEF1 = 9.00, J = 0.658; tLEF1 = 21.00, J = 0.926). To enhance reproducibility, LEF1 expression was subsequently evaluated dichotomously (positive/negative). Positivity in tLEF1 and nLEF1 staining was strongly associated with WNT-AG ($p = 0.003$ and $p < 0.001$, respectively). However, pLEF1 positivity, when WNT-AG cases were excluded, was insufficient to differentiate between SHH-AG and G3/4 ($p = 0.196$).

When comparing the staining patterns of β-catenin and LEF1 for identifying WNT-AG, nLEF1 demonstrated superior sensitivity and specificity compared to β-catenin (Table 3).

For ROR2, the tROR2 and cROR2 H-scores were significantly lower in G3/4 tumors ($p = 0.008$ and $p = 0.043$, respectively). When evaluated dichotomously, tROR2 negativity was significantly associated with

**TABLE 3.** Efficiency of β-catenin and LEF1 Staining Patterns in Determining WNT-AG.

| | | WNT-AG (n) | Non-WNT (n) | *p* value | Sensitivity | Specificity | PPV | NPV |
|---|---|---|---|---|---|---|---|---|
| tLEF1 | (+) | 11 | 44 | 0.003 | 100.00% | 45.67% | 20.00% | 100.00% |
| | (-) | 0 | 37 | | | | | |
| nLEF1 | (+) | 11 | 3 | < 0.001 | 100.00% | 96.29% | 78.57% | 100.00% |
| | (-) | 0 | 78 | | | | | |
| pLEF1 | (+) | 9 | 44 | 0.077 | 81.82% | 45.67% | 16.98% | 94.87% |
| | (-) | 2 | 37 | | | | | |
| β-catenin | (+) | 10 | 4 | < 0.001 | 83.33% | 95.12% | 71.43% | 97.50% |
| | (-) | 2 | 78 | | | | | |

LEF1, lymphoid enhancer-binding factor 1; tLEF1, total LEF1; nLEF1, nuclear LEF1; pLEF1, punctate LEF1; WNT-AG, WNT activated group; PPV, positive predictive value; NPV, negative predictive value.

G3/4 ($p = 0.01$), whereas no significant difference was observed between molecular subgroups for cROR2 ($p = 0.094$).

Cyclin D1 H-scores were significantly higher in WNT-AG cases ($p < 0.001$). Optimal cut-off analysis for identifying WNT-AG indicated a relatively low threshold for Cyclin D1 (H-score = 4.50, J = 0.574), similar to LEF1. When assessed dichotomously, Cyclin D1 positivity was significantly more frequent in WNT-AG tumors ($p = 0.001$).

Analysis of concordance among ROR2, LEF1, and Cyclin D1 revealed no correlation between ROR2 staining and the other markers. Cyclin D1 showed a moderate correlation with tLEF1, nLEF1, and pLEF1 H-scores ($p < 0.001$), higher H-scores in β-catenin-positive cases ($p = 0.003$), and a low-degree correlation with YAP1 H-scores ($p = 0.001$).

### Evaluation of cases undergoing EPIC array methylation analysis

Methylation analysis using the EPIC array was performed on 29 selected cases. Of these, 9 cases were classified as WNT-AG (31.03%), 8 as SHH-AG (27.59%), 6 as G3 (24.14%), and 6 as G4 (24.14%).

Following methylation analysis, the molecular subgroups of cases initially categorized as medulloblastoma–not otherwise specified (MB-NOS) were clarified. In five cases with immunohistochemically ambiguous molecular profiles, the methylation-based classification differed from the initial diagnosis.

Regarding nLEF1 expression, all WNT-AG cases demonstrated positivity, whereas all G3 cases were negative. One G4 case showed nLEF1 positivity. In addition, two nLEF1-positive cases were classified as SHH-AG; both had low calibration scores (0.38). In these three cases, nLEF1 H-scores were notably low (2, 15, and 30, respectively). Prior to methylation analysis, these cases were classified as MB-NOS because they were positive for β-catenin and GAB1. Despite the low calibration scores, these cases were ultimately classified as SHH-AG based on concordant IHC profiles, histopathological features, and radiological findings consistent with this subgroup. When the two cases with a calibration score of 0.38 were excluded, the specificity of nLEF1 increased to 98.73%, and the positive predictive value (PPV) increased to 91.67%, compared with the values reported in Table 3.

Overall, nLEF1 positivity was significantly associated with identification of the WNT-AG subgroup ($p < 0.001$). Although the mean pLEF1 H-score was higher in SHH-AG cases than in other molecular groups, this difference did not reach statistical significance for molecular subgroup discrimination.

Evaluation of tROR2 and cROR2 expression revealed negativity in only three G3 cases, with a statistically significant association ($p = 0.014$). However, comparison of ROR2 H-scores across molecular groups did not demonstrate significant differences.

A statistically significant difference was observed among molecular subgroups with respect to Cyclin D1 positivity ($p = 0.009$). Cyclin D1 positivity was detected in 8 WNT-AG cases (88.89%), 5 SHH-AG cases (62.50%), 1 G3 case (16.67%), and 1 G4 case (16.67%). Consistent with these findings, Cyclin D1 H-scores were highest in WNT-AG cases, and this difference was statistically significant ($p = 0.006$).

### Recurrence and survival findings

A total of 77 cases with a postoperative follow-up duration of at least 2 months were evaluated for disease progression. The median follow-up period was 25 months (range, 2–140 months). Disease progression occurred in 35 cases (45.45%). At the 3-year follow-up, progression was observed in 24 cases (31.17%), increasing to 28 cases (36.36%) at 5 years.

Survival data were available for 92 cases. Three patients died due to postoperative complications and were excluded from survival analyses; thus, 89 cases were included. The median survival follow-up was 45 months (range, 2–154 months). Overall, 33 patients (37.08%) died during the follow-up period. Mortality rates were 24.72% (22 patients) at 3 years and 28.09% (25 patients) at 5 years.

Univariate analysis revealed no statistically significant differences in progression-free survival (PFS) among molecular subgroups ($p = 0.206$). Similarly, no significant associations were observed between tLEF1 or pLEF1 positivity and overall PFS. However, in the 3-year PFS analysis, pLEF1 positivity was associated with improved progression outcomes ($p = 0.038$). At 5 years, positivity for both tLEF1 and pLEF1 correlated with significantly longer PFS ($p = 0.049$ and $p = 0.036$, respectively).

Multivariate Cox regression analyses incorporating age, sex, cerebrospinal fluid metastasis, Chang stage, and clinical risk group demonstrated that tLEF1 and pLEF1 positivity remained independently associated with prolonged PFS ($p = 0.002$ and $p = 0.019$, respectively; Figure 5). In the 3-year multivariate model, only pLEF1 retained statistical significance ($p = 0.006$). In contrast, both tLEF1 ($p = 0.001$) and pLEF1 ($p = 0.005$) remained significant predictors of improved PFS in the 5-year model. No significant associations with PFS were identified for nLEF1, Cyclin D1, tROR2, or cROR2 in any analysis.

Overall survival (OS) differed significantly among molecular subgroups ($p = 0.001$). Patients with SHH-AG exhibited the most favorable survival outcomes, whereas those with Group 3/4 tumors demonstrated poorer survival. These associations remained unchanged in multivariate analysis.

In univariate OS analyses, none of the LEF1 staining patterns—tLEF1, nLEF1, or pLEF1—showed a significant association with survival. However, in the 3-year OS analysis, positivity for both tLEF1 and pLEF1 was associated with improved survival ($p = 0.024$ and $p = 0.049$, respectively). At 5 years, tLEF1 remained significantly associated with better OS ($p = 0.042$), whereas the association for pLEF1 was of borderline significance ($p = 0.087$).

Multivariate analyses were performed using the same covariates included in the PFS model. In these analyses, positive expression of nLEF1 and tLEF1 remained independently associated with improved OS ($p = 0.037$ and $p = 0.044$, respectively; Figure 5). In the 3-year multivariate model, only tLEF1 retained statistical significance ($p = 0.010$), whereas nLEF1 ($p = 0.983$), pLEF1 ($p = 0.061$), and Cyclin D1 ($p = 0.055$) were not significant. In the 5-year multivariate model, both tLEF1 ($p = 0.008$) and nLEF1 ($p < 0.001$) were significantly associated with improved survival, while pLEF1 ($p = 0.069$) and

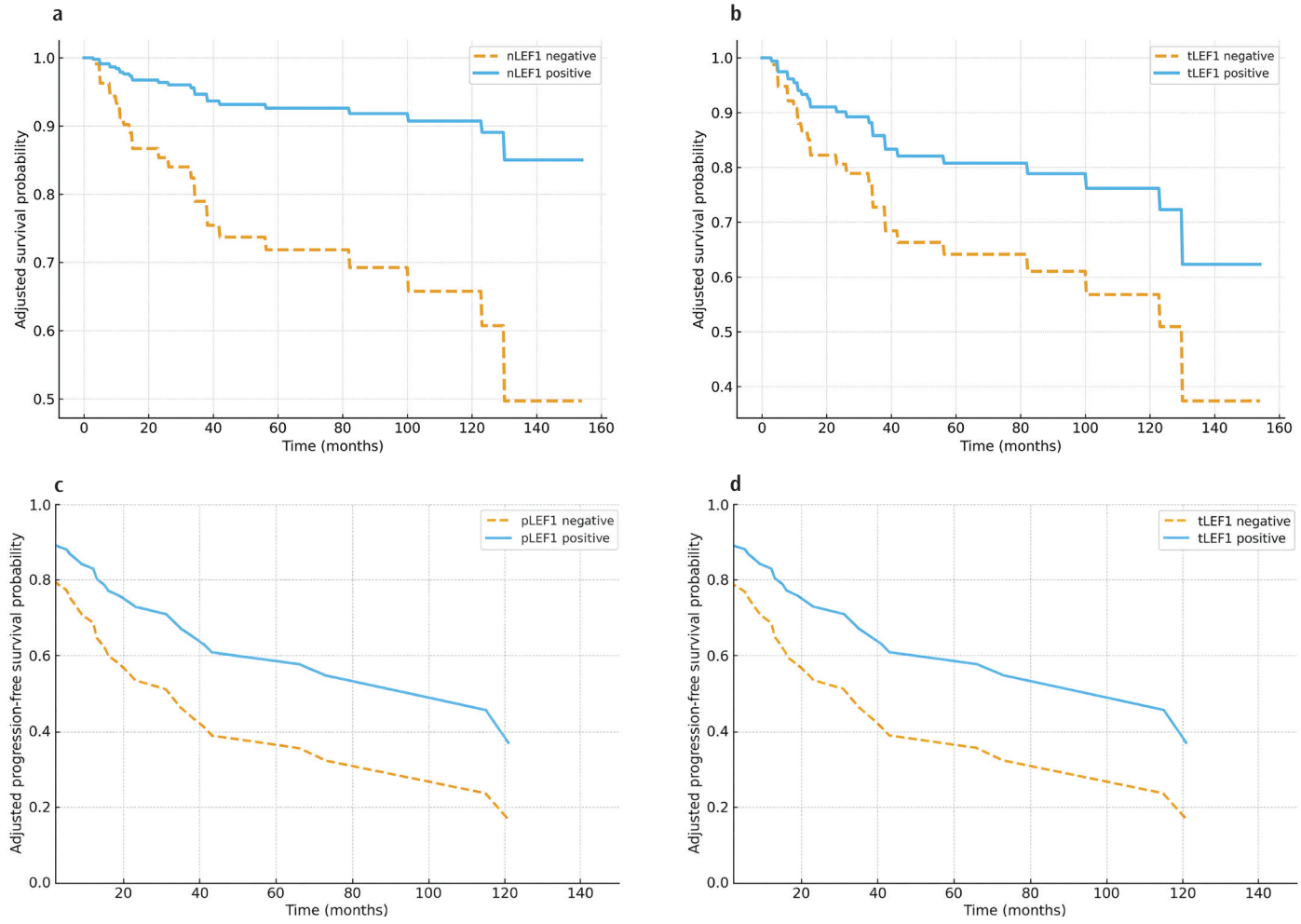


**FIG. 5.** Cox-adjusted survival curves. nLEF1 overall survival curve (a). tLEF1 overall survival curve (b). pLEF1 progression-free survival curve (c). tLEF1 progression-free survival curve (d).

*tLEF1, total lymphoid enhancer-binding factor 1; nLEF1, nuclear LEF1; pLEF1, punctate LEF1.*

Cyclin D1 ($p = 0.049$) demonstrated borderline associations. No significant associations with OS were observed for tROR2 or cROR2 in any analysis.

## DISCUSSION

In laboratories where molecular and genetic techniques are unavailable, accurate classification of medulloblastoma molecular subgroups remains challenging. Although IHC markers capable of reliably distinguishing between G3 and G4 tumors have yet to be established, even the markers currently used to identify SHH-AG and WNT-AG subgroups present considerable difficulties in terms of evaluation and interpretation. Given the markedly different prognoses associated with these molecular subgroups and the well-recognized challenges in interpreting β-catenin IHC for the identification of WNT-AG, we sought alternative diagnostic approaches.

Large-scale studies have reported that the relative frequencies of WNT-AG, SHH-AG, and G3/4 medulloblastomas range from approximately 6–11%, 26–28%, and 61–67%, respectively.[11-14] In the present study, the proportion of WNT-AG cases was consistent with these previously reported distributions; however, notable differences were observed in the frequencies of SHH-AG and G3/4 tumors. This discrepancy may be explained by several factors, including our institution's tendency to perform surgical intervention more frequently in SHH-AG medulloblastomas, which are often well circumscribed, differences in the age distribution of surgically treated patients, and, importantly, the inherent limitations imposed by the relatively small sample size.

While molecular subgroup assignments were generally consistent with GAB1, YAP1, and β-catenin markers, we observed notable discrepancies. Specifically, eight GAB1-positive cases were classified as WNT-AG and six as G3/4, while three β-catenin-positive cases were assigned to SHH-AG and one to G3/4. These findings suggest that IHC methods alone cannot reliably determine molecular subgroups. Consequently, in the absence of genomic or methylation analyses, molecular group classification should be interpreted in conjunction with clinical, radiological, and demographic data. Our results

align with those of Min et al.,[12] who reported limitations of GAB1 positivity in identifying SHH cases, even when using catenin beta 1 (*CTNNB1*) gene mutation analysis and array-based techniques.

Interpreting β-catenin staining remains challenging for many neuropathologists. To address this, we investigated LEF1 staining patterns as an alternative marker for identifying WNT-AG. Strong nLEF1 staining was consistently associated with WNT-AG. When comparing nLEF1 and β-catenin, nLEF1 demonstrated higher sensitivity and PPV for WNT-AG, while both markers exhibited similar specificity. These results indicate that nLEF1 is a highly promising indicator of WNT pathway activation in medulloblastoma.

Additionally, we observed that punctate, weak pLEF1 staining H-scores correlated with GAB1 H-scores, with higher pLEF1 scores in SHH-AG compared with G3/4. These findings suggest that the pLEF1 staining pattern may serve as a useful marker for SHH-AG.

To date, the only study examining the relationship between LEF1 staining and molecular subgroups in medulloblastoma is that of Wang et al.[15] They performed LEF1 and β-catenin immunostaining on 30 cases and analyzed the results using whole-exome sequencing. LEF1 expression was observed in eight cases: three classified as WNT-AG and five as SHH-AG. Diffuse LEF1 expression corresponded with WNT-AG, whereas focal expression was linked to SHH-AG. Although Wang et al.[15] did not report the pLEF1 staining pattern we identified, their findings—showing LEF1 staining correlates with WNT-AG and SHH-AG and is absent in G3/4—are consistent with our results.

Our data indicated that ROR2 is an inadequate marker for identifying WNT-AG medulloblastoma. The only prior study examining ROR2 expression in medulloblastoma, conducted by Lee et al.,[7] suggested that ROR2 expression is associated with a favorable prognosis. The authors also reported higher ROR2 mRNA levels in cases with *CTNNB1* mutations, suggesting potential co-activation of canonical and non-canonical WNT pathways. In our cohort, negative ROR2 staining appeared to be indicative of G3/4 tumors. Among the 29 cases subjected to methylation analysis, only three were ROR2-negative, all of which were classified as G3. Further studies are required to draw definitive conclusions regarding the role of ROR2.

Cyclin D1 was also more frequently positive in WNT-AG cases and exhibited relatively higher H-scores. Its staining pattern was consistent with β-catenin and LEF1, reflecting its role in the WNT signaling pathway. Although Cyclin D1 often displayed focal and low H-scores, which complicates evaluation, it may serve as a useful adjunct marker for identifying WNT-AG. These observations align with a limited body of literature. Yu et al.[16], Yu and Li[17] reported correlations among β-catenin, LEF1, and Cyclin D1 expression in medulloblastoma, and Rogers et al.[18] observed a near-significant association between β-catenin and Cyclin D1.

The 3- and 5-year OS and PFS rates in our cohort were consistent with published data.[19-23] SHH-AG was associated with a favorable prognosis, whereas G3/4 cases had poor outcomes. Contrary to previous studies, WNT-AG did not demonstrate a statistically significant difference from other groups in our analysis. This discrepancy may be attributable to the small number of WNT-AG cases and the inclusion of a few untreated patients, which may have limited the statistical power.

Previous studies have reported that LEF1 is associated with poor prognosis in solid tumors.[23] However, our study is the first to specifically evaluate LEF1 in relation to recurrence and survival in medulloblastoma. Multivariate analysis revealed that nLEF1 and tLEF1 were associated with favorable OS, whereas pLEF1 and tLEF1 correlated with improved PFS. Although additional studies are required before LEF1 can be adopted as a routine prognostic biomarker, its ease of assessment and strong predictive potential suggest that it may serve as a promising indicator independent of molecular subgroup classification.

The use of "EPIC array" methylation analysis represents a major strength of this study, providing high-quality data on recurrence, survival, and other clinical parameters. Nevertheless, the inability to perform methylation analysis for all cases—and the consequent challenge of evaluating G3 and G4 separately—constitutes a limitation. This limitation restricted our ability to fully elucidate the relationship between these subgroups and the IHC markers examined. Although it did not substantially affect our primary objective of differentiating WNT-AG from other molecular groups, it partially constrained our capacity to assess G3 and G4 individually. Additionally, within the subset of cases analyzed by methylation profiling, this limitation hindered further validation of the potential role of ROR2 staining in distinguishing between G3 and G4. Future studies could be strengthened by increasing sample size and incorporating multicenter data, thereby enabling methylation analysis across the entire cohort.

Another limitation of our study is the lack of data on interobserver reproducibility for the LEF1 staining patterns we defined (nLEF1 and pLEF1). Wang et al.[15] classified these patterns as diffuse and focal, whereas we applied a different evaluative approach. As these staining patterns are assessed by a larger number of observers and validated in further studies, their reliability and clinical applicability are expected to become better established.

The findings of this study support the routine use of nLEF1 staining in combination with β-catenin for identifying WNT-AG, particularly in laboratories with limited access to molecular genetic methods. Further comprehensive studies examining the relationship among nLEF1 expression, β-catenin, and WNT-AG are anticipated to improve the accuracy of molecular subgroup classification in routine diagnostic practice and contribute to more precise clinical management of patients. Additionally, if confirmed in future studies, Cyclin D1 may serve as a Supplementary Table marker alongside these two.

pLEF1 may aid in identifying SHH-AG in conjunction with established markers such as GAB1, OTX2, Filamin A, and YAP1, which are routinely used in diagnostic workflows. Although no IHC method currently differentiates between G3 and G4 subgroups, further research on ROR2 is warranted. Our ultimate aim is to enhance the management, treatment, and follow-up of patients with medulloblastoma, even in the absence of methylation analysis or genome sequencing.

**Acknowledgements:** We extend our sincere gratitude to Mücahit Özkelle and Dilanur Kamalı for their invaluable technical assistance. We declare that there are no conflicts of interest or external funding sources to disclose for this study.

**Ethics Committee Approval:** This study was approved by the Clinical Research Ethics Committee of the Faculty of Medicine, Marmara University (approval number: 09.2021.1253; date: 05.11.2021).

**Informed Consent:** The requirement for informed consent was waived due to the retrospective nature of the study.

**Data Sharing Statement:** The data that support the findings of this study are available from the corresponding author upon reasonable request.

**Authorship Contributions:** Concept- M.F.T., D.G., N.E., A.D., Y.B., F.B., B.M.A., S.U.B.; Design- M.F.T., D.G., S.U.B.; Supervision- S.U.B.; Materials- D.G., N.E., A.D., Y.B., F.B., B.M.A.; Data Collection or Processing- M.F.T., D.G., N.E., A.D., Y.B., F.B., B.M.A.; Analysis and/or Interpretation- M.F.T., B.M.A.; Literature Review- M.F.T.; Writing- M.F.T., S.U.B.; Critical Review- B.M.A., S.U.B.

**Conflict of Interest:** The authors declare that they have no conflict of interest.

**Funding:** The authors declared that this study received no financial support.

**Supplementary Table:** https://www.balkanmedicaljournal.org/img/files/BalkanMedJ-2025-10-51-supplement.pdf

## REFERENCES

1. Ostrom QT, Cioffi G, Gittleman H, et al. CBTRUS statistical report: primary brain and other central nervous system tumors diagnosed in the United States in 2012-2016. *Neuro Oncol.* 2019;21:v1-v100. [CrossRef]
2. Louis DN, Perry A, Wesseling P, et al. The 2021 WHO Classification of Tumors of the Central Nervous System: a summary. *Neuro Oncol.* 2021;23:1231-1251. [CrossRef]
3. Bailey P, Cushing H. Medulloblastoma Cerebelli: A common type of midcerebellar glioma of childhood. *Archives of Neurology & Psychiatry*. 1925, 14:192-224.
4. Millard NE, De Braganca KC. Medulloblastoma. *J Child Neurol.* 2016;31:1341-1353. [CrossRef] Erratum in: *J Child Neurol.* 2016:0883073816670445. [CrossRef]
5. Paterson E, FarR RF. Cerebellar medulloblastoma: treatment by irradiation of the whole central nervous system. *Acta Radiol (Stockh).* 1953;39:323-336. [CrossRef]
6. Rutka JT, Hoffman HJ. Medulloblastoma: a historical perspective and overview. *J Neurooncol.* 1996;29:1-7. [CrossRef]
7. Lee SE, Lim SD, Kang SY, Suh SB, Suh YL. Prognostic significance of Ror2 and Wnt5a expression in medulloblastoma. *Brain Pathol.* 2013;23:445-453. [CrossRef]
8. Theresia E, Malueka RG, Pranacipta S, et al. Association between Ki-67 labeling index and histopathological grading of glioma in Indonesian population. *Asian Pac J Cancer Prev.* 2020;21:1063-1068. [CrossRef]
9. Hasbay B, Kayaselcuk F, Suner HI, Sarialioglu F. Medulloblastoma: clinicopathological correlates of SHH, WNT, and Non-WNT/SHH molecular subgroups analysis and prognostic significance: mono-institutional series. *Turk Neurosurg.* 2022;32:595-602. [CrossRef]
10. Caliskan I, Lu R, Szu Lyn Ding C, Sadala de Souza F, Perry A, Tihan T. Searching for a cut-off point for p53 immunohistochemistry as evidence of TP53 mutations. *Free Neuropathol.* 2024;5:6. [CrossRef]
11. Kool M, Korshunov A, Remke M, et al. Molecular subgroups of medulloblastoma: an international meta-analysis of transcriptome, genetic aberrations, and clinical data of WNT, SHH, Group 3, and Group 4 medulloblastomas. *Acta Neuropathol.* 2012;123:473-484. [CrossRef]
12. Min HS, Lee JY, Kim SK, Park SH. Genetic grouping of medulloblastomas by representative markers in pathologic diagnosis. *Transl Oncol.* 2013;6:265-272. [CrossRef]
13. Schwalbe EC, Lindsey JC, Nakjang S, et al. Novel molecular subgroups for clinical classification and outcome prediction in childhood medulloblastoma: a cohort study. *Lancet Oncol.* 2017;18:958-971. [CrossRef]
14. Waszak SM, Northcott PA, Buchhalter I, et al. Spectrum and prevalence of genetic predisposition in medulloblastoma: a retrospective genetic study and prospective validation in a clinical trial cohort. *Lancet Oncol.* 2018;19:785-798. [CrossRef]
15. Wang D, Gong J, Zhang H, et al. Immunohistochemical staining of LEF-1 is a useful marker for distinguishing WNT-activated medulloblastomas. *Diagn Pathol.* 2022;17:69. [CrossRef]
16. Yu J, Ji G, Shi W, et al. RBM5 acts as tumor suppressor in medulloblastoma through regulating Wnt/β-catenin signaling. *Eur Neurol.* 2020;83:242-250. [CrossRef]
17. Yu J, Li H. The expression of FAT1 is associated with overall survival in children with medulloblastoma. *Tumori.* 2017;103:44-52. [CrossRef]
18. Rogers HA, Miller S, Lowe J, Brundler MA, Coyle B, Grundy RG. An investigation of WNT pathway activation and association with survival in central nervous system primitive neuroectodermal tumours (CNS PNET). *Br J Cancer.* 2009;100:1292-1302. [CrossRef]
19. Jiang T, Zhang Y, Wang J, et al. A retrospective study of progression-free and overall survival in pediatric medulloblastoma based on molecular subgroup classification: a single-institution experience. *Front Neurol.* 2017;8:198. [CrossRef]
20. Johnston DL, Keene D, Strother D, et al. Survival following tumor recurrence in children with medulloblastoma. *J Pediatr Hematol Oncol.* 2018;40:e159-e163. [CrossRef]
21. Thompson EM, Hielscher T, Bouffet E, et al. Prognostic value of medulloblastoma extent of resection after accounting for molecular subgroup: a retrospective integrated clinical and molecular analysis. *Lancet Oncol.* 2016;17:484-495. [CrossRef] Erratum in: *Lancet Oncol.* 2022;23:e59. [CrossRef]
22. Weil AG, Wang AC, Westwick HJ, et al. Survival in pediatric medulloblastoma: a population-based observational study to improve prognostication. *J Neurooncol.* 2017;132:99-107. [CrossRef]
23. Yang X, Liu H, Ye T, Ye Z. High expression of LEF1 correlates with poor prognosis in solid tumors, but not blood tumors: a meta-analysis. *Biosci Rep.* 2020;40:BSR20202520. [CrossRef]